

Electro-Hydrodynamics of Semi-Conductive Fluids: With Application to Electro-Spraying

11/29/04 CWH

Background

It has long been known that strong electric fields can disrupt liquid surfaces. One particularly useful application of this observation has been the development of electro-spray-ionization (ESI) systems. The basic concept is to eject liquid from a nozzle connected to a voltage source that has a relatively high electric potential compared to its surroundings. When adjusted for certain operating conditions, a thin jet of liquid is ejected from the nozzle that subsequently breaks up into charged droplets having a relatively uniform size. There are many useful industrial applications for a system that produces small droplets of specified size; particularly if the droplets don't coalesce because of their electrical repulsion. Having a charge also means that these drops can be electrically deflected toward a target. This technology, for example, has been advantageously applied to paint spraying, atomization of fuels, printing, mass spectroscopy and a variety of spray drying processes.

In this note we describe an extension to the *FLOW-3D*[®] computational fluid dynamics software that gives it a mechanism for simulating the electro-hydrodynamic behavior of semi-conducting fluids. The new capability is illustrated and validated by application to a simple laboratory bench test and to the formation of Taylor cones, the principal component in ESI systems.

Approach

Computation of electric potentials and dielectric forces in *FLOW-3D*[®] has previously been reported (FSI-00-TN52(Rev10/01) and FSI-01-TN56). Here we focus on changes introduced when fluid is permitted to have some electrical conductivity, κ .

Free electric charge per unit volume in a fluid, ρ_e , is described by the conservation equation,

$$\frac{\partial \rho_e}{\partial t} + \nabla \cdot (\mathbf{u} \rho_e) = -\nabla \cdot (\kappa \mathbf{E}). \quad (1)$$

Here Ohm's law has been used to relate the electric current to the conductivity and electric field, $\mathbf{j} = \kappa \mathbf{E}$. The presence of a charge density influences the electric field according to

$$\nabla \cdot (\varepsilon_0 \varepsilon \mathbf{E}) = \rho_e + \rho_o. \quad (2)$$

In this expression ε_0 is the permittivity of free space and ε is the dielectric constant (i.e., relative permittivity) and ρ_o is a charge density coming from other sources such as solid mass particles in a fluid. Free charge density also contributes to the electrical force per unit volume acting on the fluid,

$$\mathbf{F} = \rho_e \mathbf{E} + \frac{1}{2} \varepsilon_0 (\varepsilon - 1) \nabla E^2 \quad (3)$$

The first term (called electrophoresis) arises from the free charge while the second term (called dielectrophoresis) arises from polarization effects. In a fluid with very small conductivity there is little or no free charge and only the second term can have an influence on the fluid dynamics. On the other hand, if a liquid has sufficient electrical conductivity that free charge accumulates only at its surface, the resulting force is sometimes referred to as electro-capillarity.

In the present case we are most interested in semi-conductive liquids in which the conductivity is large enough to allow some free charge to accumulate at liquid surfaces. However, we do not restrict the free charge to exist only at surfaces, for when the relaxation of charge density within a liquid is not fast enough with respect to fluid-dynamic time scales there can be a more general charge distribution.

Another way to write the force in Eq.(3), which some investigators prefer, is through the Maxwell stress tensor, T_{ij} , where (using index notation in which repeated indices are summed)

$$F_i = \nabla_k T_{ik},$$

$$T_{ik} = \varepsilon E_i E_k - \frac{1}{2} \delta_{ik} \varepsilon E^2 \quad (4)$$

If free charge accumulates at a free liquid surface it induces a normal component of electric field, E_n , at the surface. According to the Maxwell stress tensor this results in normal and tangential stresses acting on a liquid surface given by,

$$T_n = \frac{1}{2} \varepsilon_0 E_n^2, \quad T_t = \varepsilon_0 E_n E_t. \quad (5)$$

Typically, the normal stress tends to disrupt a surface if it is large enough to overcome the stabilizing effects of surface tension. From Eq.(5) we see that the tangential stress is important only when there is an additional tangential component of the electric field. Surface tangential stresses are interesting because they induce convective flows and fluid deformations that cannot be generated by distributed body forces.

Finally, we note that highly conducting liquids cannot support significant tangential electric fields so that electro-hydrodynamics in this limit is not as interesting. These observations, then, support our emphasis here on the electro-hydrodynamics of semi-conducting fluids where normal and tangential surface stresses induce some interesting fluid dynamic processes.

Additions to the **FLOW-3D**[®] software

With the exception of Eq.(1), all the machinery for computing electric fields and electric forces already exist in the software so it is only necessary to add the charge density equation, Eq.(1), plus including this charge on the right side of Eq.(2).

In constructing a numerical approximation for Eq.(1) it is useful to see the form of this equation in the interior of a liquid where both the conductivity and dielectric properties are constant. In this case the right side of Eq.(1) can be converted, using Eq.(2) and ignoring ρ_0 , to a term proportional to the charge density,

$$\frac{\partial \rho_e}{\partial t} + \nabla \cdot (\mathbf{u} \rho_e) = -\frac{\kappa}{\epsilon_0 \epsilon} \rho_e \quad (6)$$

The right hand side implies there is an exponential decay in the charge density at any point in the interior of a conducting liquid, with a characteristic relaxation time of $\tau = \epsilon_0 \epsilon / \kappa$. Because the permittivity ϵ_0 in the numerator of τ is very small (e.g., 8.854×10^{-12} in SI units) charge decay is usually very fast, unless the conductivity appearing in the denominator is also very small.

When an explicit approximation is used to numerically model Eq.(6) the decay term imposes a limit on the size of the time step, $\delta t < 2\tau = 2\epsilon_0 \epsilon / \kappa$, that cannot be exceeded without suffering a computational instability. This stability limit can be quite restrictive unless the conductivity is sufficiently small. To overcome this limitation we have introduced an implicit formulation for Eq.(1) that eliminates the explicit stability condition without having to perform a computationally expensive iterative solution.

An example of the utility of the implicit formulation is given in the next section that describes a validation problem having both theoretical and experimental data with which to make comparisons. The problem was first published by Melcher and Taylor to show how tangential stresses on a semi-conducting liquid can induce a significant fluid flow. The liquid in the test had a dielectric constant of 10.0. In the first computations we performed an explicit method was used with a liquid conductivity of 8.05×10^{-6} S/m. According to the above stability condition, this computation would have produced nonsense if the time-step size exceeded 2.2×10^{-5} s. In fact, a maximum step size of 1.0×10^{-5} was used and could not be raised much above this value without the computations going crazy.

With the implicit formulation for Eq.(1) added to **FLOW-3D**[®] it has been found that the computational time-step size could be increased to the next controlling stability limit, which was $\delta t = 8.12 \times 10^{-3}$ s, several orders of magnitude larger. Computations that had originally taken more than an hour were reduced to approximately a minute, a clear demonstration of the usefulness and greater robustness of the implicit formulation.

Validation Test

The Leaky-Dielectric model defined by Melcher and Taylor (J.R. Melcher and G.I. Taylor, "Electrohydrodynamics: A Review of the Role of Interfacial Shear Stresses," Ann. Rev. Fl. Mech., 111, 1969) has been found useful for a variety of important applications including electro-spraying. In their proposed model a fluid is assumed to be weakly conducting to the extent that a bulk charge density does not exist, but a surface charge density can develop at fluid interfaces. Under such conditions the application of an electric field having a component tangential to an interface will result in tangential stresses acting on the fluid.

To demonstrate this model Melcher and Taylor (MT) constructed a simple laboratory test that consisted of a shallow, conducting liquid in a container with electrodes at either end. At one end the electrode was extended above the liquid surface to form a tilted cover, which generated a tangential component of the electric field at the liquid surface. This

field in conjunction with conductivity in the liquid generated a tangential surface stress that drives a counter-clockwise circulatory flow in the liquid pool, Fig.1.

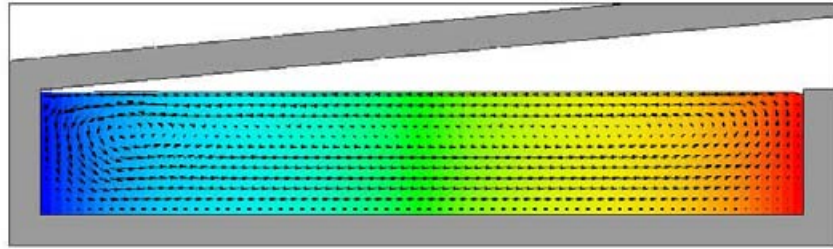


Figure 1. Computed flow field in Melcher-Taylor apparatus. Color indicates electric potential.

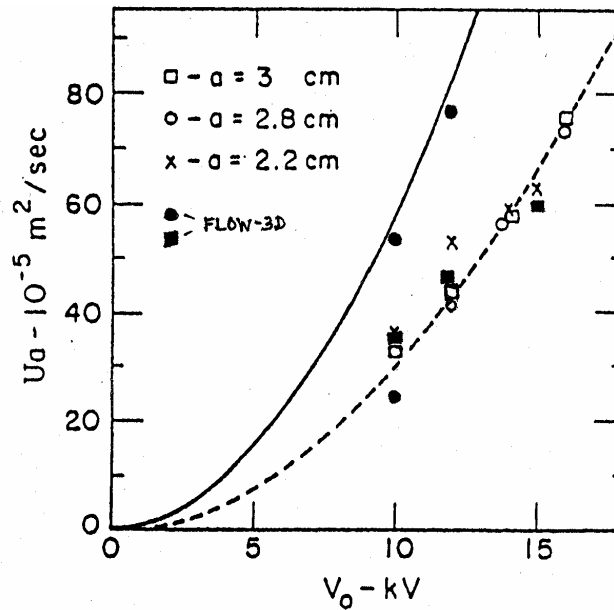


Figure 2. Comparison of computations (solid dots and squares), theory (solid line) and experimental data (other symbols and dashed line). Plot shows the product of maximum electrode spacing and the interfacial velocity as a function of the applied potential. Figure taken from Melcher-Taylor paper cited in text; *FLOW-3D* data are plotted as solid symbols.

Figure 2 shows results reproduced from the MT paper. The solid line represents a simplified theoretical prediction for the tangential surface velocity (times the tilt-height of the lid) at the mid point of the tank versus applied voltage. Experimental results from a variety of tests are indicated by crosses and open squares through which a dashed line has been drawn. The fact that theory indicates higher fluid speeds than experiment was attributed by MT to flow losses at the ends of the tank, which were not considered in the theory.

Our computations show that the real reason for the difference between theory and experiment is that the experiments used a low liquid conductivity, reported to be approximately $1.0e-11$ S/m. This value is too small to satisfy the conditions of the MT

Leaky-Dielectric theory. To see this we first simulated the device using a relatively large conductivity of $\kappa=8.05e-6S/m$ (about six orders of magnitude larger than in the experiment). This produced the top most data point (solid circle) at 10kV, which is quite close to the theoretical prediction (solid line). The large conductivity insures that any charges in the liquid are only found at the liquid surface, in line with the Leaky-Dielectric assumption.

When the conductivity is reduced to $\kappa=1.0e-11S/m$ the approximate value reported by MT for the experiments, our computations give the bottom most data point at 10kV (solid circle). In this case the computational result is a little below the experimental data. Because the precise value of conductivity was uncertain we raised the value to $\kappa=3.0e-11S/m$, which is still quite small. Computational results with this value fall right into agreement with the experimental data, i.e., the solid square plotted at 10kV.

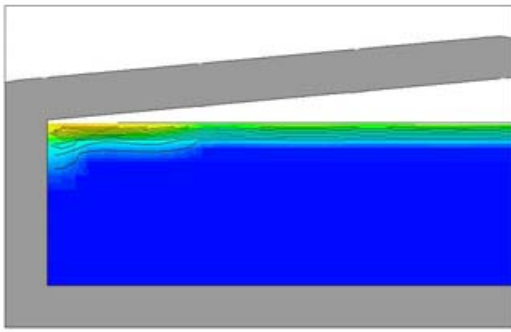


Figure 3. Charge distribution with low conductivity. Some charge has been advected down from the surface at the left side.

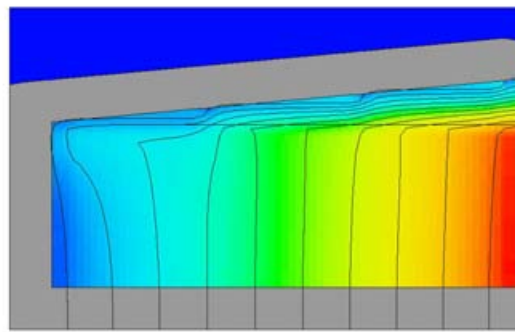


Figure 4. Equipotential lines show distortion at left because of charge generated in conducting liquid.

The smaller value of conductivity allowed some charge to exist below the liquid surface at the left end of the tank, Fig.(3). This charge is seen to modify the electric potential at the left end as well, Fig.(4).

Additional computations using $\kappa=8.05e-6S/m$ and higher potentials of 12kv and 15kv produced results close to the theoretical curve (solid circles; at 15kv the point is off scale at 116.6). Using the lower value of $\kappa=3.0e-11S/m$ with higher voltages of 12vk and 15kv produced results that remain close to the experimental values (solid squares at 12kv and 15kv).

All computations used the same 2D grid of 78 by 23 cells and ran quickly on the order of 1 to 2 minutes for each simulation.

We may conclude from this example that the addition of fluid conductivity to **FLOW-3D**[®] works well and extends the Leaky-Dielectric model because charges are not confined to liquid surfaces. The later feature produces excellent agreement between experimental observations and computations.

Application to Taylor Cones

In a classic paper G.I. Taylor (“Disintegration of Water Drops in an Electric Field,” Proc. R. Soc. Lon. A **280**, 383 (1964)) described how electric fields can distort liquid drops and in some circumstances produce a thin liquid jet emanating from a drop. Now referred to as Taylor cones, these jet flows have found uses for a wide variety of applications that require a stream of more-or-less uniform droplets having an electric charge.

To demonstrate the usefulness of the new conducting fluid model two sample Taylor cone simulations have been performed. An axisymmetric arrangement was used that consisted of a nozzle of inside diameter $7.0e-4\text{m}$ that is charged to 6000 volts. Downstream $25.0e-4\text{m}$ there is located a grounded plate perpendicular to the axis of the nozzle with a central hole of diameter $3.0e-4\text{m}$. A flow of liquid into the bottom of the nozzle has a fixed axial velocity of 0.02m/s . The properties of the liquid are: density= 827.0kg/m^3 , viscosity 0.0081kg/m/s , dielectric constant= 10.0 , surface tension= 0.0235N/m , and conductivity= $8.05e-6\text{S/m}$.

The computational grid selected for this test consisted of 30 radial cells and 220 axial cells. A minimum radial cell size of $0.8e-5\text{m}$ was used at the axis of symmetry. The total time simulated was 0.03s , which required a CPU time of 36.5 minutes on a laptop computer having a 1.6GHz Pentium 4 processor chip. Initially liquid was even with the top of the nozzle. The jet forms explosively at about $t=0.017\text{s}$ and then slowly evolves into a smaller diameter jet as it approaches a near steady state condition.

Steady conditions, however, were not quite reached since there continued to be a small, steady increase in the liquid volume in the computational region. Presumably, a slightly smaller flow rate into the nozzle would have brought the flow to a steady state.

Figure 5a shows the cross section of the computed Taylor cone. The jet has a maximum axial velocity of approximately 4.34m/s and exhibits small perturbations in diameter that move up and down its length. It appeared that the jet might be trying to reduce its mean diameter, but it was pushing the resolution of the grid since the minimum jet radius observed is only about 1.5 grid cells in thickness.

A close-up of the flow distribution in the cone (where only every other velocity vector in each direction has been plotted) is given in Fig.6. There is no recirculation in this case, contrary to observations by some researchers (e.g., Barrero, et al, J.Electrostatics, **47**, 13 (1999)). Instead, it is interesting to note the change in the radial profile of axial velocity. At the exit of the nozzle the velocity is largest at the axis, as would be expected with Poiseuille flow in the nozzle. Approximately one nozzle radius downstream from the exit there is almost no radial variation in axial velocity. Further downstream the profile is reversed with the minimum axial velocity at the axis and the largest at the surface of the liquid. It is the rapid increase in surface velocity that leads to the drawing out of liquid into a jet.

Jet formation is graphically illustrates the importance of tangential stresses applied to surface charges by an electric field. With the relatively high conductivity used in this case surface charges are confined to the liquid surface as shown in Fig.7.

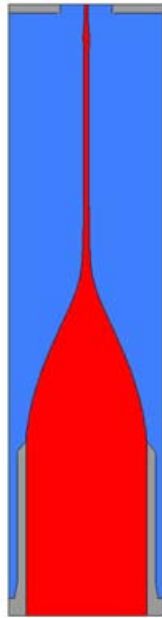


Figure 5a. Taylor cone with 6kv potential.

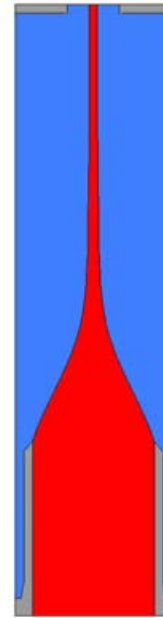


Figure 5b . Taylor cone with 8kv potential.

A repeat of the simulation with the potential of the nozzle raised from 6kv to 8kv produced the Taylor Cone shown in Fig.5b. Higher field strengths produce a shorter cone with a larger cone angle at the base of the jet. This is in agreement with observations by Hayati, et al (I. Hayati, A.I. Bailey and Th.F. Tadros, J. Colloid Inter. Sci. **117**, 205 (1987)).

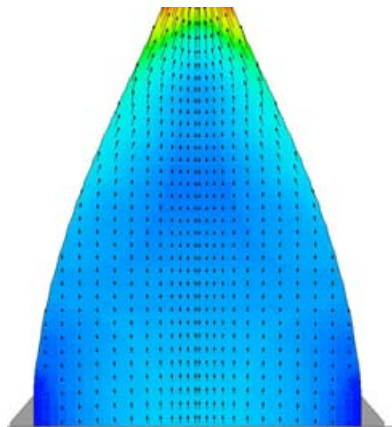


Figure 6. Flow distribution in cone region.



Figure 7. Charge distribution on surface.

Acknowledgement

This work has been based on work by Dr. Jun Zeng of Coventor who nicely demonstrated how to put a Leaky Dielectric model into **FLOW-3D**[®].